# Polyfluorene-Based Light-Emitting Rod−Coil Block Copolymers

**Su Lu,[†] Tianxi Liu,[‡] Lin Ke,[†] Dong-Ge Ma,[§] Soo-Jin Chua,[†] and Wei Huang*,[‡]**

*Institute of Materials Research and Engineering (IMRE), National University of Singapore, 3 Research Link, Singapore 117602, Republic of Singapore; Institute of Advanced Materials (IAM), Fudan University, 220 Handan Road, Shanghai 200433, People's Republic of China; and Changchun Institute of Applied Chemistry, Chinese Academy of Sciences, 109 Renmin Street, Changchun 130022, People's Republic of China*

*Received February 6, 2005; Revised Manuscript Received July 2, 2005*

ABSTRACT: A series of novel well-defined polyfluorene-based rod−coil copolymers have been synthesized for application in light-emitting diodes (LEDs). These polymers were prepared by using polyfluorene macroinitiators to initiate the atom transfer radical polymerization of 2-(9-carbazolyl)ethyl methacrylate (CzEMA). The incorporation of CzEMA block successfully created energy transfer, and the findings showed that intramolecular energy transfer dominates in solution while intermolecular energy transfer plays a more important role in solid state. It was also demonstrated that energy transfer is more efficient for the block copolymers with respect to the corresponding polymer blends. Better spectral stability has been demonstrated with these copolymers in comparison to PF homopolymer through annealing studies. Interesting self-assembled nanostructures were observed for these polymers, which is dependent on the polymer composition. Electrochemical characterization indicated that the presence of the carbazole effectively raises the HOMO level with respect to the polyfluorene homopolymer, suggesting better hole injection properties. Preliminary LED experiments with these polymers indicated enhanced device performance compared to polyfluorene (PF) homopolymer. The results implied that rod−coil block copolymers with optoelectronic functionality are promising candidates for blue LED applications in terms of the suppression of green emission.

## Introduction

Conjugated polymers have attracted much interest in light-emitting diodes (LEDs) due to cost-effective processablity, excellent stability, high efficiency, and easy color-tuning.[1] To achieve optimal device performance, it has been crucial to develop novel optoelectronic materials with different electronic functionalities because most electroluminescent polymers exhibit unbalanced carrier injection and transportation properties. Several strategies have been pursued to address such an issue, including making polymer blends[2] and copolymers.[3]

Recently, rod−coil block copolymers which consist of conjugated segments connected with flexible segments have been the subject of extensive studies due to their unusual morphologies and photophysical behavior in both solution and solid state.[4,5] For optoelectronic applications, however, it is important to endow the flexible coils with optoelectronic functionalities. As such, a combination of complementary virtues from both rod and coil blocks can be envisioned. The approach suppresses the unfavorable macrophase separation encountered in many polymer blends while presents unique microphase separation with the formation of highly ordered geometries or patterns at nanoscales, which may lead to additional electronic processes such as exciton confinement and interfacial effects.[6] The photophysical properties can also be tuned through charge-transfer and energy-transfer interactions by selecting the proper luminescent segments. Most recently, a diblock copolymer architecture has been suggested to benefit the electroluminescence more than its homopolymer and alternating copolymer counterparts.[7] Therefore, preparation of rod−coil copolymers opens a new channel to manipulate the optoelectronic properties of conjugated materials.

Polyfluorenes (PFs) have been known as the most promising blue-light-emitting polymers due to their excellent chemical, thermal, processing, and emission properties.[8] Unfortunately, the performance of PF homopolymer is limited by the poor hole injection properties. Hole-transporting (HT) units, such as triarylamine and carbazole, have been integrated into the PF backbones to balance the injection of both carriers.[3f,9] End-capping PF main chain with HT moieties has also proven effective.[10] However, as an alternative approach, PF-based rod−coil block copolymers containing hole-transporting flexible segments have been rarely studied.[11] This inspired the employment of a carbazole-containing poly(2-(9-carbazolyl)ethyl methacrylate) (PCzEMA) as the flexible block. Actually, PCzEMA shows similar optoelectronic properties in many aspects to its analogy, poly(vinylcarbazole) (PVK),[12] which has been extensively used as hole transporting material and energy transfer donor in LED devices.[13] In addition, PCzEMA would be able to be polymerized by atom transfer radical polymerization (ATRP), which has been proven efficient to prepare well-defined PF-based block copolymers in our previous work.[14] In this paper, we extend our previous studies to prepare well-defined PCzEMA−PF−PCzEMA triblock copolymers under ATRP conditions (Scheme 1). Spectroscopic, electrochemical, morphological, and electroluminescent properties of these copolymers are investigated. The results suggest that, by integrating carbazole functionality into a rod−coil block copolymer structure, we have been able

[†] National University of Singapore.
[‡] Fudan University.
[§] Chinese Academy of Sciences.
* To whom correspondence should be addressed: Tel +86 21 5566 4188; Fax +86 (21) 6565 5123; e-mail wei-huang@fudan.edu.cn.

10.1021/ma050267o CCC: $30.25 
Published on Web 09/02/2005

**Scheme 1. Synthesis Route of the PF−PCzEMA Block Copolymers**

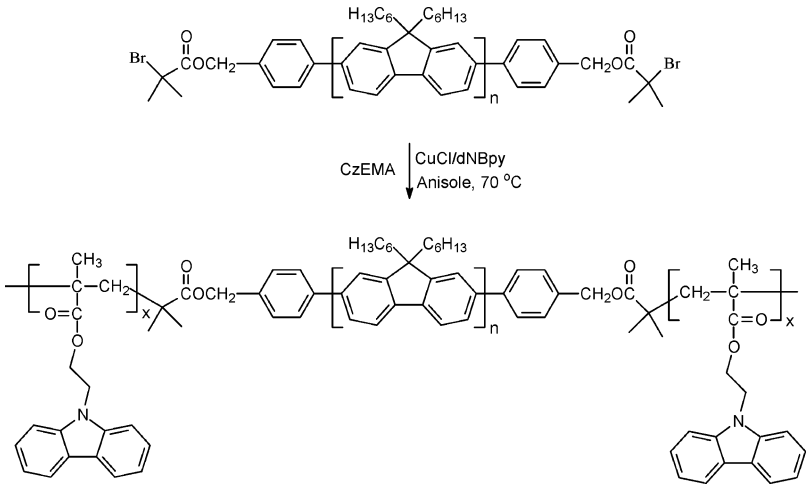


**Table 1. ATRP Results of CzEMA Homopolymers and Block Copolymers[a,b]**

| samples | [M]/[I] | M/S (w/v)[c] | temp (°C) | time (min) | conv (%) | $M_n$ (theor) | $M_n$ (NMR) | $M_n$ (SEC) | $M_w/M_n$ |
|---|---|---|---|---|---|---|---|---|---|
| PCzEMA1 | 40 | 3:5 | 70 | 60 | 90 | 10 000 | | 6 700 | 1.18 |
| PCzEMA2 | 40 | 1:1 | 70 | 50 | 80 | 9 000 | | 6 500 | 1.13 |
| **A** | 20 | 2:5 | 75 | 150 | 95 | 8 300 | 8 600 | 8 600 | 1.31 |
| **B** | 31 | 3:8 | 75 | 80 | 93 | 10 900 | 9 900 | 9 200 | 1.32 |
| **C** | 80 | 2:3 | 70 | 110 | 86 | 22 200 | 24 400 | 16 600 | 1.19 |
| **D** | 139 | 1:1 | 70 | 70 | 87 | 36 700 | 33 900 | 23 400 | 1.18 |
| **E** | 40 | 2:5 | 90 | 75 | 93 | 14 300 | 16 400 | 13 000 | 1.44 |
| **F** | 60 | 2:5 | 75 | 180 | 85 | 19 700 | 20 100 | 15 900 | 1.30 |

[a] [dNBpy]:[CuCl]:[I] = 4:2:1. [b] **MI-1** ($M_n$ = 3000) was used for **A**, **B**, **C**, and **D**; **MI-2** ($M_n$ = 6000) was used for **E** and **F**. [c] Ratio of monomer vs solvent (g/mL).

to improve the hole-injection property while maintaining the essential spectral features of PF which is critical to blue emission. The observed ordered nanostructures of the block copolymers via self-assembly allow further optimization of device performance at a supramolecular level.

## Results and Discussion

**Synthesis and Characterization of Copolymers.** The PF macroinitiators were prepared through Yamamoto condensation of 9,9-dihexyl-2,7-dibromofluorene monomer and 4-bromobenzyl alcohol end-capper at either 2:1 or 5:1 ratio.[14b] Esterification of the above product with 2-bromoisobutyryl bromide afforded final PF macroinitiators. The structures of the macroinitiators were confirmed by $^1$H NMR, $^{13}$C NMR, and FTIR. The number-average molecular weight ($M_n$) was determined to be about 3000 and 6000 (corresponding to macroinitiator **MI-1** and **MI-2**, respectively) with typical polydispersity index (PDI) of 1.5−1.65.

Initially, ATRP of CzEMA was investigated by using molecular initiator, ethyl 2-bromoisobutyrate, in anisole with 4,4′-(5-nonyl)-2,2′-bipyridine (dNBipy) and CuCl as the catalytic system. The monomer conversion reached 90% within 1 h at 70 °C. The resulting PCzEMA presented molecular weights close to the theoretical values and narrow PDI as shown in Table 1, indicating the essentially controlled nature of the ATRP reaction. Therefore, similar ATRP conditions were used to prepare the block copolymers with the macroinitiators at different monomer−initiator ratios. The polymerization results are summarized in Table 1. Generally, high conversion of the polymerization could be achieved within a relatively short reaction period. Figure 1 shows the typical size exclusion chromatography (SEC) profiles

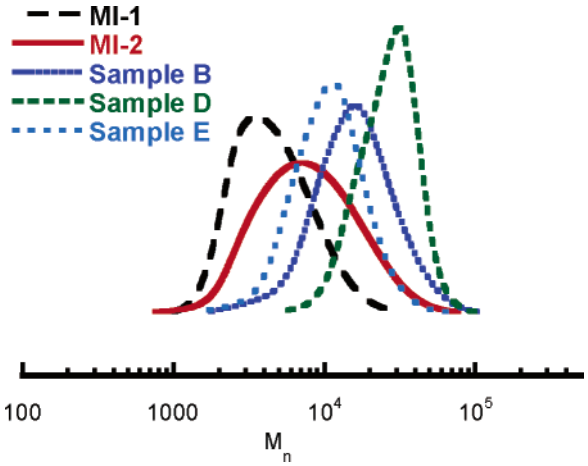


**Figure 1.** SEC profiles of PCzEMA−PF−PCzEMA block copolymers.

of the PCzEMA−PF−PCzEMA triblock copolymers (PF−PCzEMA) and the PF macroinitiators (**MI-1** and **MI-2**). The detector responses corresponding to the PF macroinitiator residues are negligibly weak, implying that the macroinitiator has been integrated into the block structures. The molecular weights determined by $^1$H NMR are close to the theoretical values and also corresponding reasonably to the SEC values. The PDI of the block copolymers has narrowed to less than 1.4 as compared with those of the macroinitiaors, which also indicates the formation of the well-defined block structures. Table 1 summarizes the ATRP results of CzEMA.

The chemical structures of the PF−PCzEMA block copolymers were confirmed by $^1$H NMR, $^{13}$C NMR, and FTIR spectroscopy. Representative $^1$H NMR and $^{13}$C NMR spectra of PF−PCzEMA block copolymers are shown in Figure 2. The results strongly suggest the

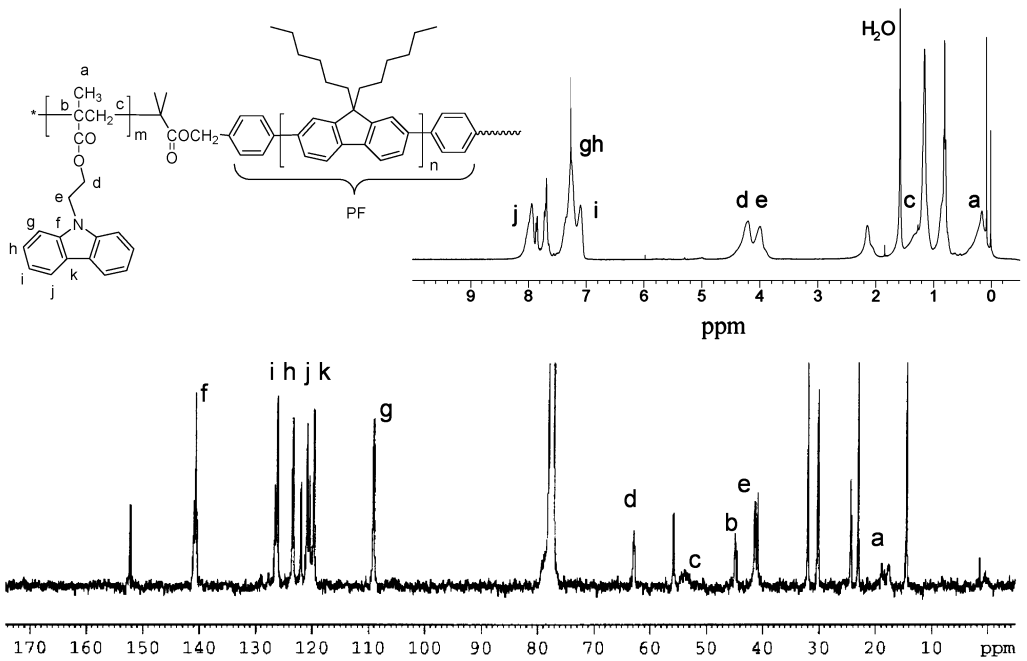


**Figure 2.** $^{1}H$ NMR (top) and $^{13}C$ NMR (bottom) spectra of PF−PCzEMA block copolymer. The unsigned peaks are from PF segments.

formation of well-defined block copolymers through ATRP with efficient initiation of PCzEMA and perfect intactness of PF backbone. The polymer composition can thus be estimated by comparing the relative integration of the peak from 3.7 to 4.5 ppm and the peak at 2.2 ppm, assigned to the two methylene groups (−C**H**$_2$−C**H**$_2$−) in PCzEMA groups and the two methylene groups at the 9-position of the fluorene ring, respectively. Both $^{1}H$ NMR and $^{13}C$ NMR spectra of PF−PCzEMA follow linear superposition of those of the macroinitiator and PCzEMA.

**Photophysical Properties.** The representative UV−vis and emission spectra of PF−PCzEMA in $CHCl_3$ are shown in Figure 3. The solution absorption spectra are close to the weight-averaged sum of the respective absorbance of both segments, implying the desired composition has been achieved. The copolymers do not exhibit any new bands in the absorption spectra, indicating that there is no observable interaction between the two components in their ground states. The fluorescence spectra and efficiencies (excitation at 383 nm) of the block copolymers in $CHCl_3$ are comparable to those of PF homopolymers, suggesting that the photoluminescence properties of PF are not influenced by the PCzEMA segments.

When comparing absorption and emission spectra of PF macroinitiator **MI-1** with a PCzEMA homopolymer (Figure 3c), one can see that the emission spectrum of PCzEMA and the absorption spectrum of PF overlap significantly from which donor−acceptor energy transfer from PCzEMA to PF can be expected. Note that the maximum of the absorption of PF is located at the low-energy side of the emission band of PCzEMA, which may facilitate the energy transfer because the red-shifted emission species tend to have longer lifetime.[15] In fact, the photoexcitation of carbazole chromophores at 343, 332, 294, and 262 nm created apparently identical predominant emission with that excited at 383 nm (Figure 3d). No new emission features were observed in the wavelength range of 300−700 nm, implying that intermolecular exciplex can be ruled out in solution. The energy transfer between the two components was also probed by photoluminescent excitation (PLE) spectra. As depicted in Figure 3d, the PLE spectrum measured at 415 nm as a function of the excitation wavelength has been normalized in the range of 370−400 nm where only PF absorbs. The PLE spectrum showed similar spectral features to the corresponding absorption, indicating that both PF and PCzEMA contribute the emission. However, when the excitation wavelength blue-shifts, the relative intensity in the PLE spectra with respect to the absorption bands decreases significantly. Therefore, the transitions from higher excited states may be accompanied by enhanced possibility of nonradiative quenching. Similar observation has been reported by Lemmer et al. in a study of the photophysical behavior of ladder-type poly(*p*-phenylene) (PPP) in solid state.[16]

It has been found that energy transfer is incomplete in solution with weak residue fluorescence at 345−365 nm from carbazole chromophores (Figure 3b). The energy transfer in the solution can be quantitatively studied by investigating the quenching of the donor fluorescence (PCzEMA) in the presence of the acceptor (PF).[17] It can be seen that the efficiency decreases significantly when the PCzEMA segments in the block copolymers becomes longer (Figure 3b inset). To elucidate the incomplete energy transfer, a mixture of PCzEMA homopolymer and macroinitiator **MI-1** in chloroform with a weight ratio of 3:1 was used as a control sample. The PL excitation spectrum was identical to that of **MI-1** and did not exhibit any signal from PCzEMA, in distinct contrast to the block copolymer with the same composition. Therefore, the singlet excited states yielded in the simple mixture are only caused by the direct photoexcitation of the PF segment. This result unambiguously demonstrates an intrachain energy transfer involved in the emission of the block copolymers. We suggest that singlet energy migration along PCzEMA occurs when it is irradiated at the wavelength corresponding to the absorption of carbazole.[18] Excited energy migration between carbazole

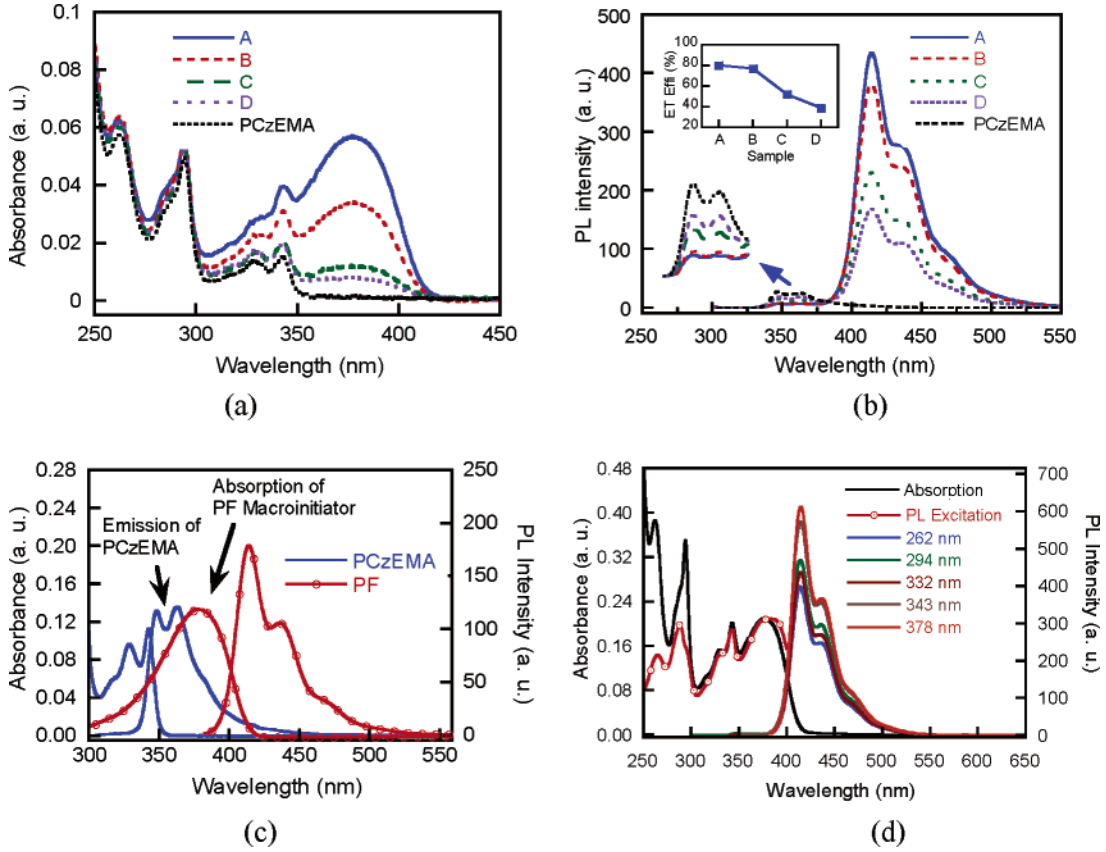


**Figure 3.** (a) UV and (b) PL spectra (excitation at 294 nm) of PCzEMA and PF−PCzEMA in $CHCl_3$. Inset: energy-transfer efficiency of the samples. (c) Spectral overlap of PCzEMA and PF. (d) UV, PL, and PLE of copolymer **B**.

chromophores has been described previously due to relatively large Förster radius for self-transfer.[19] However, in solution, intrachain long-range energy transfer may be difficult for such a coiled polymer with linear architecture due to low local chromophore density.[20] The exciton may emit or be quenched through other depopulation channels prior to transfer to the PF sites, especially for copolymers with longer PCzEMA coils. Similar results have been obtained recently in a study of porphyrin dendrimers.[21]

The absorption and emission spectra (excitation at 294 nm) of the block copolymers in solid state are shown in Figure 4a,b. Both the absorption and emission spectra are almost identical with those measured in solution. However, the fluorescence residue of PCzEMA has been completely distinguished in solid state. All the samples give strong blue emission peaked at 419 nm, similar to that of PF homopolymers. The energy transfer from carbazole chromophore to PF is very efficient even for polymer **D** with the highest content of PCzEMA. In addition, excitation of **D** at 294 nm creates fluorescence almost 3 times stronger than at 377 nm, indicating that the intensity of the sensitized emission is even stronger than that of a direct PF emission. Therefore, sensitization of the chromophore by the telechelic antenna is more efficient than direct excitation at the absorption maximum. It should be pointed out that although **MI-1**/PCzEMA blends also exhibit more efficient energy transfer in solid state than in solution, the fluorescence residue is significantly stronger than that of the corresponding copolymers (Figure 4b inset). We suggest that in solid state excitonic interchain migration dominates the energy transfer, which facilitates the exciton migration to achieve long-range energy migration.[20] It is noteworthy that interchain energy transfer has recently been viewed more important than the intrachain fashion.[22] Because of possible inhomogeneous distribution of PF in the blends as a result of phase separation at large scales, the fluorescence quenching of PCzEMA is less efficient in comparison to the block copolymer architectures.[23]

PF has previously been suggested to form exciplex with pendent carbazole moiety in a graft configuration, which showed significant red-shifted emission in solid state, even for freshly prepared films.[24] For the copolymers, however, photoexcitation of the films only generated well-resolved emission spectra similar to those in solution. Therefore, PF and PCzEMA segments in a block architecture may not interact at a molecular level. In other words, they may form independent microphases. Annealing experiments were also performed to investigate the spectral stability of these block copolymers. Figure 4c shows the normalized PL emission spectra of the films of the copolymers and a poly(9,9-dihexylfluorene-2,7-diyl) (PFH) homopolymer annealed at 150 °C in air for 2 h. It can be seen that, in contrast to PFH, the green emission has been successfully suppressed for the copolymers. The results are consistent with the previous findings that the optical stability of PF could be improved in polymer blends.[25] Recently, formation of fluorenone caused by photooxidation during annealing has been demonstrated.[26a,b] Further studies suggested that fluorenone excimers be the essential reason for the spectral instability of PF.[26c] The enhanced spectral stability of the copolymers compared to PF homopolymer could be partially ascribed to the surrounding PCzEMA coils which may shield the PF segments from oxidation. In addition, since PF has been diluted by

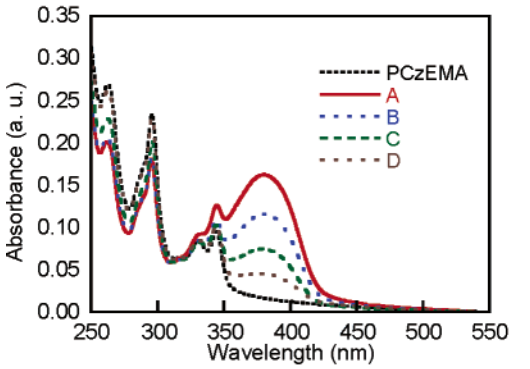


(a)

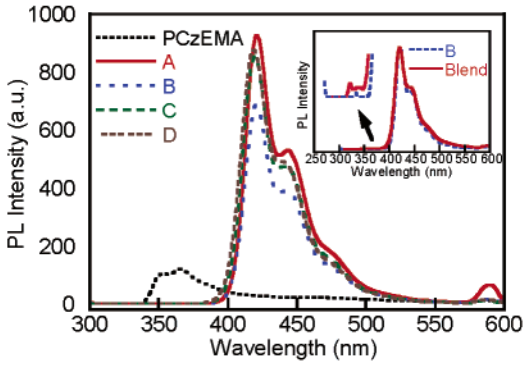


(b)

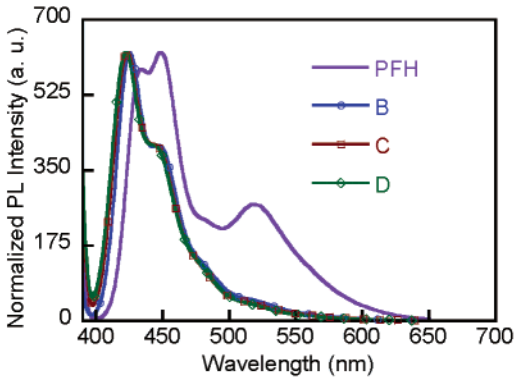


(c)

**Figure 4.** (a) UV and (b) PL spectra (excitation at 294 nm) of PCzEMA and PF−PCzEMA in solid state. Inset: PL of **B** vs the corresponding blend. (c) Normalized PL spectra (excitation at 380 nm) of thin films of **B**, **C**, and **D** as well as PFH annealed at 150 °C in air for 2 h.

PCzEMA to some extent in the copolymers, the formation of fluorenone excimers would be suppressed. The PCzEMA may also act as an energy barrier to hinder excitonic migration from polyfluorene to fluorenone excimer sites. As a consequence, the green emission will be minimized in the case of the copolymers. It is important to note, however, that significant decrease of emission intensity of the copolymers after annealing was observed even though the green emission was insignificant. Therefore, the formation of intrachain fluorenone sites can be expected which do not contribute to the green emission.[26c]

**Thermal Properties and Morphologies.** The thermal properties of the polymers were determined by differential scanning calorimetry (DSC). No crystallization and melting peaks were detected for all samples, indicating that these materials are amorphous. While PCzEMA exhibits a $T_g$ at 122 °C, those of the copolymers with different PF blocks are between 126 and 130 °C. Although block copolymers composed of two incompatible components usually present two $T_g$s, the $T_g$ of PF block was not detected probably due to relatively short PF chains. Actually, the PF macroinitiators did not show any $T_g$ during DSC measurements, either.

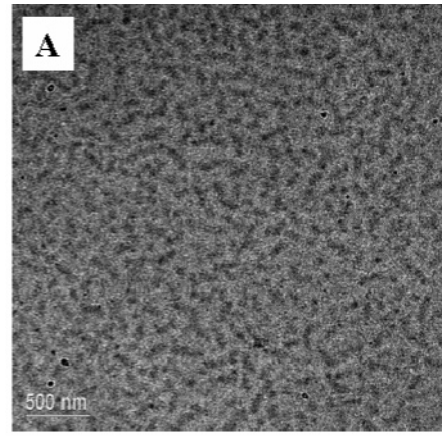


(a)

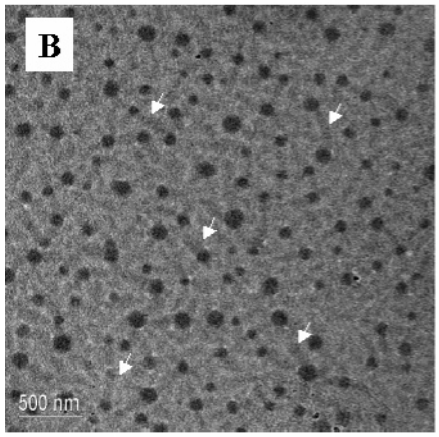


(b)

**Figure 5.** TEM images of block copolymer films: (a) **B** and (b) **D**.

TEM was employed to study the morphology of solid films of the block copolymers, as shown in Figure 5a,b. Sufficient "phase contrast" is obtained by a proper amount of objective lens defocus in the bright-field mode of TEM. It can be seen that, upon evaporation of the chloroform, copolymer **B** forms wormlike morphology (dark regions) with a relatively uniform worm diameter of about 45 ± 5 nm (Figure 5a), while typical spherical micelles or aggregates (darker regions with higher electron density) with rather nonuniform and larger diameter of about 115 ± 30 nm are observed for copolymer **D** (Figure 5b). Close inspection on TEM image of copolymer **D**, however, shows that the individual spherical micelles are "connected" by wormlike structures with light contrast (indicated by white arrows) to form a unique network morphology. We suggest that the isolated aggregates are tending to coalesce together to form complex morphologies by further self-assembly,[27] especially at the later stage of the film

deposition due to higher solution concentrations. Similar observations on such self-association behavior have also been observed in some amphiphilic block copolymer systems recently.[28]

It is important to note that the rigid PF segments in copolymers **D** and **B** have the same molecular weight. However, the molecular weight of copolymer **D** is much higher (about 3.4 times) than that of copolymer **B**. Therefore, the dark regions with higher electron density in the TEM micrographs presumably consist of both rod and coil segments, as evidenced by the increased diameter of aggregates with the length of PCzEMA coil block. Such observations indicate that, given the length of rigid PF segments is fixed (as studied in present case), increasing the length of flexible PCzEMA segments probably favors the formation of large spherical micelles (here, for sample **B**), while the presence of short coil block is apt to form wormlike structures (here, for sample **D**). It should also be pointed out that the observed morphologies do not change significantly even after annealing at 100 °C for several hours. The relatively stable nanostructures with excellent optical properties are of potential use in optoelectronic devices. Further detailed studies will be conducted on the effects of different film-forming conditions (such as solution concentration, (selective) solvents used, solvent evaporation speed, and so on) on the growth of the nanostructured morphologies and control of optical properties such as energy transfer.

**Electrochemical Characterization.** The cyclic voltammograms (CV) of homopolymer PCzEMA and block copolymers **E** and **MI-2** are shown in Figure 6a. The electrochemical signals of the block copolymer follow the superposition of those of the individual blocks, suggesting that both PCzEMA and PF serve as independent electroactive species in the block copolymer. A partially reversible process can be observed with an oxidation peak at 1.59 V and the corresponding reduction peak at 1.26 V which has been assigned to the PF component. The onset potential shifts to 1.15 V, about 0.2 V lower than that of PF homopolymer. The slightly increased oxidation potential of the block copolymer (0.06 V higher with respect to the PF homopolymer) may be caused by heterogeneous elecron-transfer kinetics.[29] Figure 6b shows the CVs obtained through continuing scans of the block copolymer to 1.3 V. The peak current corresponding to the dimer cationic radical increases continuously, indicating that the electropolymerization of the carbazole unit gives rise to the constant growth of carbazole dimers. Carbazole units can be facilely dimerized electrochemically through oxidation to carbazole cation radicals followed by intermolecular coupling.[24a,30] Note that after electrochemical scan the onset potential of the copolymer further shifts to 0.86 V, which is significantly lower (about 0.5 V) than that of the pristine films. Accordingly, the HOMO of PF homopolymer is estimated to be 5.8 eV, while that of the block copolymer is 5.6 eV which further decreases to 5.3 eV upon cathodical scan, considering the energy level of 4.4 eV for Ag/AgCl.[8,31] The results imply that a better hole injection properties has been achieved. The carbazole units and dimers are expected to improve the hole injection properties without affecting the energy levels of PF.

Tuning of oxidation potential is crucial to improve the carrier injection properties of a conjugated polymer. Our results have demonstrated that, using block copolymer approach, one may expect an efficient engineering of the

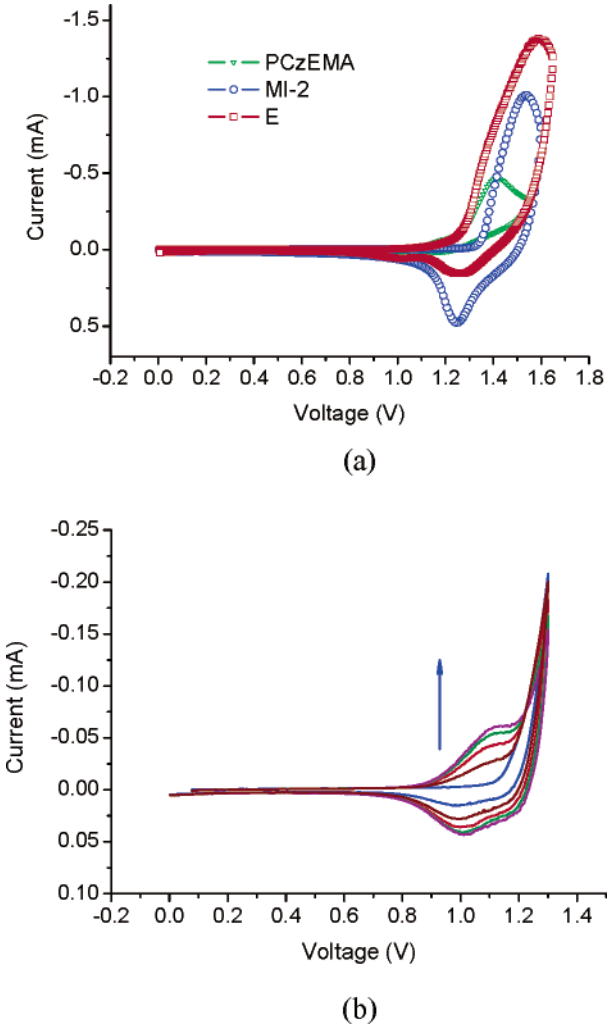


**Figure 6.** (a) CV of PCzEMA, macroinitiator **MI-2** and polymer **E** in $CH_3CN$. (b) CV of polymer **E**: sweep to 1.3 V, five cycles. The potentials are measured relative to a Ag/AgCl reference electrode.

energy levels without significantly loss of their essential electronic properties. Another advantage is that the hole-transporting properties can be further improved through electrochemical modification. In addition, the formed carbazole dimers may also serve as cross-linkers to stabilize the morphology of the block copolymers through interchain coupling. PF networks have been prepared by several groups through backbone functionalization in order to improve the morphological stability of PF and suppress the green emission.[32] As an alternative approach, electrochemical method is able to make conjugated networks for morphologically stable layers in LED.

**Electroluminescence.** Preliminary electroluminescence (EL) properties of the block copolymers were investigated with a single-layer device configuration (ITO/PEDOT:PSS/copolymers/Ca/Ag). The typical EL spectra are shown in Figure 7a. Strong blue EL emission can be observed with samples **A**, **B**, and **E**. Copolymer **B** presented slightly more low-energy emission than **E**, but the green emission has been efficiently suppressed in contrast to the carbazole-based graft copolymers reported previously.[33] The CIE coordinates are $x = 0.16$, $y = 0.13$ for copolymer **B** and $x = 0.17$, $y = 0.12$ for copolymer **E**, indicating relatively pure blue emission. It is noteworthy that, similar to the photoluminescence

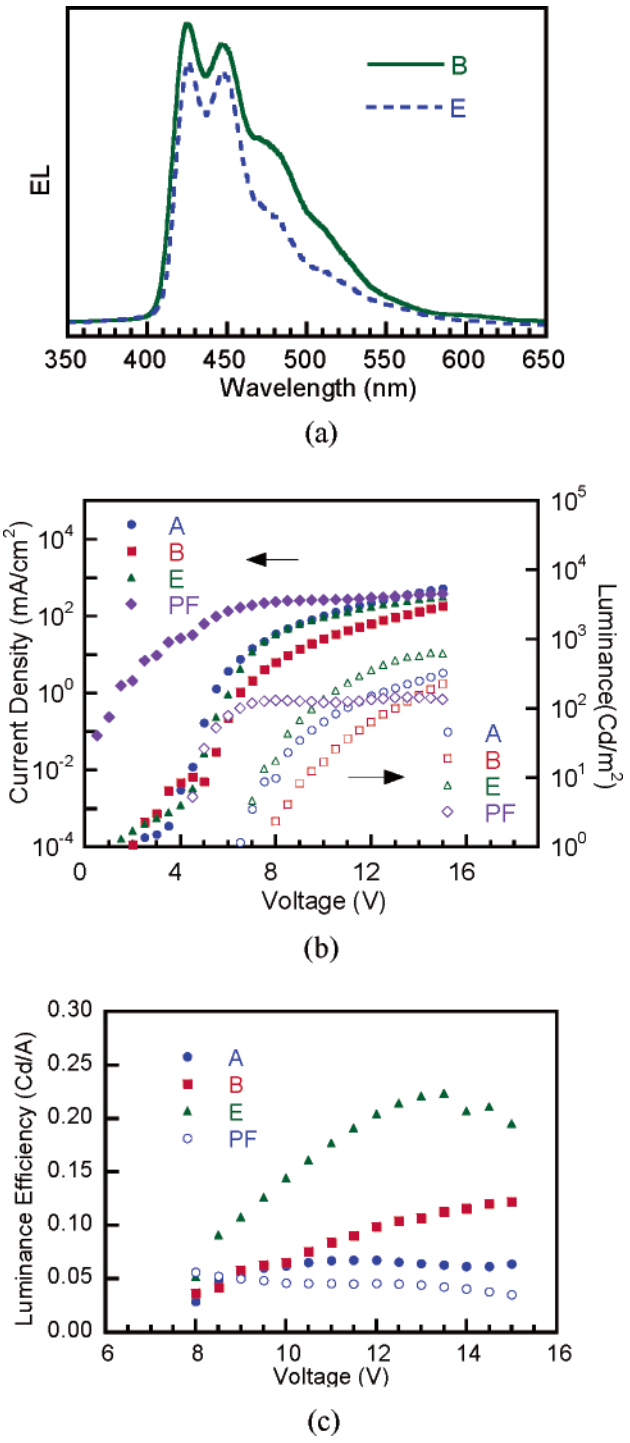


**Figure 7.** (a) Electroluminescence spectra of copolymers **B** and **E** in single-layer devices. (b) Current density and luminance and (c) electroluminscence efficiency as a function of the bias voltage in single-layer devices of copolymers **A**, **B**, and **E** and homopoloymer PFH vs voltage. Device structure: ITO/PEDOT/polymer/Ca/Ag.

in solid state, no emission from carbazole can be observed in the EL spectra. On the basis of the above observation, it is suggested that the radiative decay of excitons occurs mainly at PF due to direct carrier recombination as well as exciton migration from PCzEMA.[15] Figure 7b shows a typical $J-L-V$ relation measured from the devices fabricated with the block copolymers and PFH as comparison. For the block copolymers, the current density, $J$, starts to increase dramatically at about 3 V, and the emission is observed at about 6.5−8 V. In comparison to PFH, the current density is decreased for all devices made of copolymers. Such a decrease has been ascribed to the presence of the hole-transporting materials in PF matrix which serve as hole traps while affecting electron transport insignificantly.[2e] In addition, both the device efficiency and the maximum brightness for the block copolymers are considerably higher than those of PFH (Figure 7b,c). Considering the energy diagrams of PFH and copolymers, we suggest that the improvement in EL device performance with these block copolymers is due to the introduction of PCzEMA block which lowers the HOMO level and facilitates hole injection from anode as a consequence. It should be pointed out that the EL performance is strongly dependent on the copolymer composition. Thus, the device performance should be further enhanced by optimizing a number of the molecular parameters of the copolymers such as polymerization degree and molar percentage of the PF and PCzEMA blocks and screening more hole-transporting materials other than carbazole to make a better match of the HOMO level of the material to the work function of ITO. Understanding the relationship between film morphology and device performance is another topic of interest for us to pursue in the future.

## Conclusion

We have synthesized a series of PF-based well-defined triblock copolymers containing carbazole units through ATRP. It has been shown that, besides the interesting nanoscaled structures due to self-assembly which is not surprising for such a rod−coil copolymer system, the PF−PCzEMA copolymers by introducing electroactive carbazole into the rod−coil architecture offers a variety of new optoelectronic properties. Förster energy transfer from PCzEMA to PF in such architecture has been demonstrated. An interchain mechanism has been suggested to elucidate the energy transfer in solid state with nearly complete extinction of emission from carbazole which is ideal for LED application, in contrast to an intrachain fashion in solution. The green emission has been suppressed with the copolymers, which is explained by the dilution effect of the PCzEMA. The hole injection properties of PF have been improved successfully through the incorporation of PCzEMA segments, and electrochemical modification on these copolymers is expected to further improve the PF performance. Electroluminescence characterization presented a pure blue emission and better device performance than PF homopolymer. Therefore, these materials represent a promising class of optoelectronic polymers, based on which we may build a new platform which allows us to further explore the structure−property relationship of optoelectronic materials at a supramolecular level.

## Experimental Section

**Materials.** 2,7-Dibromofluorene (97%), 1-bromohexane (98%), 4-bromobenzyl alcohol (99%), 2-bromoisobutyryl bromide (BiBB) (98%), CuCl (99.995+%), 1,5-cycooctadiene (COD) (99%+), ethyl 2-bromoisobutyrate (98%), 4,4′-dinonyl-2,2′-dipyridyl (dNBipy) (97%), carbazole, ethylene carbonate, and bis(1,5-cyclooctadiene)nickel(0) (Ni(COD)$_2$) were purchased from Aldrich Chemical Co. Methacryloyl chloride (98%) was purchased from TCI and were used as received. *N,N*-Dimethylformamide (DMF, TEDIA, 99.9%), dichloromethane (99.9%, TEDIA), and anisole (Merck) were distilled from calcium hydride and stored under argon. Tetrahydrofuran (99.8%, TEDIA) and toluene (99.5%, Merck) were distilled from sodium/benzophenone. The

monomer 2-(carbazol-9-yl)ethyl methacrylate (CzEMA) was synthesized according to published method.[34] PF macroinitiators for ATRP were synthesized according to previously described procedure.[14b] Poly(9,9-dihexylfluorene-2,7-diyl) (PFH) was synthesized through Suzuki reaction in our lab ($M_n$ = 20K).

**Measurements.** NMR spectra were collected on a Bruker Avance 400 spectrometer with tetramethylsilane as the internal standard. FTIR spectra were recorded on a Bio-Rad FTS 165 spectrometer by dispersing samples in KBr disks. Size exclusion chromatography (SEC) analysis was conducted on a HP 1100 HPLC system equipped with the HP 1047A RI detector and the Agilent 79911GP-MXC columns, using standard polystyrene samples as the molecular weight references and THF as the eluent. UV−vis spectra were recorded on a Shimadzu 3101 spectrophotometer. The concentrations of the copolymer solutions were adjusted to about 0.01 mg/mL or less. Fluorescence measurement was carried out on a Perkin-Elmer LS 50B luminescence spectrometer with a xenon lamp as a light source. Differential scanning calorimetry (DSC) was run on a TA Instruments DSC 2920 module at a heating rate of 20 °C/min. Electrochemistry studies were performed using an Autolab PGSTAT30 potentiostat/galvanostat with a standard three-electrode electrochemical cell containing a 0.1 M tetrabutylammonium hexafluorophosphate solution in acetonitrile at room temperature under argon at a scanning rate of 100 mV/s. A platinum working electrode, platinum wire counter electrode, and an Ag/AgCl (saturated KCl and AgCl aqueous solution) reference electrode was used. The thin films for transmission electron microscopy (TEM) observation were prepared by dropping the dilute solutions (1% w/v in chloroform) onto carbon-coated copper grids. Extra solution was blotted with filter paper. After solvent evaporation, the copolymer films were directly observed using a Philips CM300-FEG TEM under an accelerated voltage of 150 kV without staining.

ITO-coated glass with a sheet resistance of 20 Ω/sq was used for LED fabrication. The routine cleaning procedure including sonication in acetone and methanol and oxygen plasma treatment was carried out. As the hole-transporting layer, a 20 nm thick poly(styrenesulfonate)-doped poly(3,4-ethylene dioxythiophene) (PEDOT) was spin-coated at a rate of 2000 rpm and an acceleration of 2000 rpm/s for 20 s on ITO. The copolymer layer of 80−100 nm was spin-coated from a solution of 10 g/L. A 20 nm thick calcium covered with a 200 nm thick silver cathode were deposited by thermal evaporation in an Edwards Auto 306 system at a base pressure of $2.0 \times 10^{-6}$ Torr. The current−luminance−voltage ($J-L-V$) curves were measured using a fully computer-controlled system consisting of a dynamic multimeter (Keithley DMM 2001), a source meter (Keithley 3A 2420), and eight calibrated Si photodiodes. The software was based on LabView. The current and luminescence output measurements were carried out by a voltage scan model. All measurements were performed in the glovebox with water and oxygen concentrations less than 1 ppm. For each of the materials, four devices were fabricated and tested, and the best data were used for discussion.

**Syntheses. a. Synthesis of PCzEMA by ATRP.** PCzEMA was synthesized by solution polymerization in anisole. In a typical run, a glass tube was charged with 0.300 g (1.07 mmol) of CzEMA, 22.1 mg (0.054 mmol) of dNBipy, and 2.7 mg (0.027 mmol) of CuCl before it was sealed with a rubber septum. The tube was degassed with three vacuum−argon cycles to remove air and moisture, and anisole (0.80 mL) was added with syringes. The glass reactor was immersed in an oil bath at 70 °C, and ethyl 2-bromoisobutyrate (5.2 mg, 26 μmol) was introduced to carry out the polymerization. After a certain period, the reaction mixture was diluted with chloroform and passed through a column of neutral alumina to remove the catalysts. The polymers were precipitated into excess of methanol and dried in a vacuum at 40 °C to afford white powder.

**b. Synthesis of PCzEMA−PF−PCzEMA Triblock Copolymers by ATRP**. The triblock copolymers were synthesized by solution polymerization in anisole. In a typical run, a glass tube was charged with 0.025 g (0.009 mmol) of PF macroinitiator, 14.7 mg of dNBipy (0.036 mmol), 0.200 g of CzEMA (0.716 mmol), and 1.8 mg (0.018 mmol) of CuCl before it was sealed with a rubber septum. The tube was degassed with three vacuum−argon cycles to remove air and moisture, and then anisole (0.20 mL) was added with syringes. The glass reactor was immersed in an oil bath at 70 °C to carry out the polymerization. After a period of time, the reaction mixture was diluted with chloroform and passed through a column of neutral alumina to remove the catalysts. The polymers were precipitated into excess of methanol and dried in a vacuum at 40 °C. Light yellow powdery to glassy samples were obtained.

**Acknowledgment.** S.L. gratefully acknowledges the National University of Singapore and the Institute of Materials Research and Engineering (IMRE) for a research scholarship and top-up award. This work was partially supported by the National Natural Science Foundation of China under Grants 60325412, 50403012, and 90406021 as well as the Shanghai Commission of Science and Technology under Grants 03DZ11016 and 04XD14002 and the Shanghai Commission of Education under Grant 2003SG03. T.X.L. also thanks the "Program for New Century Excellent Talents (NCET) in Universities" and the Shanghai "Rising-Star Program" (Grant 04QMX1403) for financial support.

## References and Notes

(1) (a) Burroughes, J. H.; Bradley, D. D. C.; Brown, A. R.; Marks, R. N.; Mackay, K.; Friend, R. H.; Burn, P. L.; Holmes, A. B. *Nature (London)* **1990**, *347*, 539. (b) Kraft, A.; Grimsdale, A. C.; Holmes, A. B. *Angew. Chem., Int. Ed.* **1998**, *37*, 402. (c) Friend, R. H.; Gymer, R. W.; Holmes, A. B.; Burroughes, J. H.; Marks, R. N.; Taliani, C.; Bradley, D. D. C.; dos Santos, D. A.; Bredas, J. L.; Logdlund, M.; Salaneck, W. R. *Nature (London)* **1999**, *397*, 121.

(2) (a) Morgado, J.; Friend, R. H.; Cacialli, F. *Appl. Phys. Lett.* **2002**, *80*, 2436. (b) Kim, J.-S.; Ho, P. K. H.; Murphy, C. E.; Friend, R. H. *Macromolecules* **2004**, *37*, 2861. (c) Grice, A. W.; Bradley, D. D. C.; Bernius, M. T.; Inbasekaran, M.; Wu, W. W.; Woo, E. P. *Appl. Phys. Lett.* **1999**, *73*, 629. (d) Chappell, J.; Lidzey, D. G.; Jukes, P. C.; Higgins, A. M.; Thompson, R. L.; O'Connor, S.; Grizzi, I.; Fletcher, R.; O'Brien, J.; Geoghegan, M.; Jones, R. A. L. *Nat. Mater.* **2003**, *2*, 616. (e) Sainva, D.; Miteva, T.; Nothofer, H. G.; Scherf, U.; Fujikawa, H.; Glowacki, I.; Ulanski, J.; Neher, D. *Appl. Phys. Lett.* **2000**, *76*, 1810. (f) Iyengar, N. A.; Harrison, B.; Duran, R. S.; Schanze, K. S.; Reynolds, J. R. *Macromolecules* **2003**, *36*, 8978. (g) Alarm, M. M.; Tonzola, C. J.; Jenekhe, S. A. *Macromolecules* **2003**, *36*, 6577.

(3) (a) Liu, B.; Yu, W.-L.; Lai, Y.-H.; Huang, W. *Chem. Mater.* **2001**, *13*, 1984. (b) Yu, W.-L.; Pei, J.; Huang, W.; Heeger, A. J. *Adv. Mater.* **2000**, *12*, 828. (c) Klärner, G.; Davey, M. H.; Chen, W. D.; Scott, J. C.; Miller, R. D. *Adv. Mater.* **1998**, *10*, 933. (d) Marsitzky, D.; Scott, J. C.; Chen, J.-P.; Lee, V. Y.; Miller, R. D.; Setayesh, S.; Müllen, K. *Adv. Mater.* **2001**, *13*, 1096. (e) Herguth, P.; Jiang, X.; Liu, M. S.; Jen, A. K.-Y. *Macromolecules* **2002**, *35*, 6094. (f) Xia, C.; Advincula, R. C. *Macromolecules* **2001**, *34*, 5854.

(4) Lee, M.; Cho, B.-K.; Zin, W.-C. *Chem. Rev.* **2001**, *101*, 3869.

(5) (a) Jenekhe, S. A.; Chen, X. L. *Science* **1998**, *279*, 1903. (b) Kong, X.; Jenekhe, S. A. *Macromolecules* **2004**, *37*, 8180. (c) Surin, M.; Marsitzky, D.; Grimsdale, A. C.; Müllen, K.; Lazzaroni, R.; Leclère, P. *Adv. Funct. Mater.* **2004**, *14*, 708. (d) Chochos, C. L.; Tsolakis, P. K.; Gregoriou, V. G.; Kallitsis, J. K. *Macromolecules* **2004**, *37*, 2502.

(6) (a) Morteani, A. C.; Dhoot, A. S.; Kim, J.-S.; Silva, C.; Greenham, N. C.; Murphy, C.; Moons, E.; Cina, S.; Burroughes, J. H.; Friend, R. H. *Adv. Mater.* **2003**, *15*, 1708. (b) Chen, X. L.; Jenekhe, S. A. *Macromolecules* **1996**, *29*, 6189.

(7) Karabunarliev, S.; Bittner, E. R. *J. Phys. Chem. B* **2004**, *108*, 10219.

(8) Neher, D. *Macromol. Rapid Commun.* **2001**, *22*, 1365.

(9) Ego, C.; Grimsdale, A. C.; Uckert, F.; Yu, G.; Srdanov, G.; Müllen, K. *Adv. Mater.* **2002**, *14*, 809.

(10) Miteva, T.; Meisel, A.; Knoll, W.; Nothofer, H. G.; Scherf, U.; Müllen, D. C.; Meerholz, D.; Yasuda, A.; Neher, D. *Adv. Mater.* **2001**, *13*, 565.

(11) Chen, J. P.; Markiewicz, D.; Lee, V. Y.; Klaerner, G.; Miller, R. D.; Scott, J. C. *Synth. Met.* **1999**, *107*, 203.
(12) Grazuleviciusa, J. V.; Strohrieglb, P.; Pielichowskic, J.; Pielichowskic, K. *Prog. Polym. Sci.* **2003**, *28*, 1297.
(13) (a) Kido, J.; Shionoya, H.; Nagai, K. *Appl. Phys. Lett.* **1993**, *63*, 2627. (b) Gong, X.; Ostrowski, J. C.; Moses, D.; Bazan, G. C.; Heeger, A. J. *J. Polym. Sci., Part B: Polym. Phys.* **2003**, *41*, 2691. (c) Chen, F.-C.; Chang, S.-C.; He, G.; Pyo, S.; Yang, Y.; Kurotaki, M.; Kido, J. *J. Polym. Sci., Part B: Polym. Phys.* **2003**, *41*, 2681.
(14) (a) Lu, S.; Fan, Q.-L.; Liu, S.-Y.; Chua, S.-J.; Huang, W. *Macromolecules* **2002**, *35*, 9875. (b) Lu, S.; Fan, Q.-L.; Chua, S.-J.; Huang, W. *Macromolecules* **2003**, *36*, 304.
(15) Brunner, K.; van Haare, J. A. E. H.; Langeveld-Voss, B. M. W.; Schoo, H. F. M.; Hofstraat, J. W.; van Dijken, A. *J. Phys. Chem. B* **2002**, *106*, 6834.
(16) Lemmer, U.; Heun, S.; Mahrt, R. F.; Scherf, U.; Hopmeier, M.; Siegner, U.; Göbel, E. O.; Müllen, K.; Bässler, H. *Chem. Phys. Lett.* **1995**, *240*, 373.
(17) Lakowicz, J. R. *Principle of Fluorescence Spectroscopy*; Kluwer Academic/Plenum Publishers: New York, 1999.
(18) (a) Watkins, D. M.; Fox, M. A. *J. Am. Chem. Soc.* **1994**, *116*, 6441. (b) Watkins, D. M.; Fox, M. A. *J. Am. Chem. Soc.* **1996**, *118*, 4344.
(19) (a) Itoh, Y.; Nakada, M.; Satoh, H.; Hachimori, A.; Webber, S. E. *Macromolecules* **1993**, *26*, 1941. (b) Keyanpour-Rad, M.; Ledwith, A.; Hallam, A.; North, A. M.; Breton, M.; Hoyle, C.; Guillet, J. E. *Macromolecules* **1978**, *11*, 1114.
(20) Webber, S. E. *Chem. Rev.* **1990**, *90*, 1469.
(21) Harth, E. M.; Hecht, S.; Helms, B.; Malmstrom, E. E.; Fréchet, J. M. J.; Hawker, C. J. *J. Am. Chem. Soc.* **2002**, *124*, 3926.
(22) (a) Beljonne, D.; Pourtois, G.; Silva, C.; Hennebicq, E.; Herz, L. M.; Friend, R. H.; Scholes, G. D.; Setayesh, S.; Mullen, K.; Bredas, J. L. *Proc. Natl. Acad. Sci. U.S.A.* **2002**, *99*, 10982. (b) Nguyen, T. Q.; Wu, J. J.; Doan, V.; Schwartz, B. J.; Tolbert, S. H. *Science* **2000**, *288*, 652.
(23) Byun, H. Y.; Chung, I. J.; Suh, Y.-S.; Shim, H. K.; Kim, D. Y.; Kim, C. Y. *Macromol. Symp.* **2003**, *192*, 151.
(24) (a) Xia, C.; Advincula, R. C. *Chem. Mater.* **2001**, *13*, 1682. (b) Xia, C.; Advincula, R. C.; Baba, A.; Knoll, W. *Chem. Mater.* **2004**, 2852.
(25) Kulkarni, A. P.; Jenekhe, S. A. *Macromolecules* **2003**, *36*, 5285.
(26) (a) List, E. J. W.; Guentner, R.; de Freitas, P. S.; Scherf, U. *Adv. Mater.* **2002**, *14*, 374. (b) Kulkarni, A. P.; Kong, X.; Jenekhe, S. A. *J. Phys. Chem. B* **2004**, *108*, 8689. (c) Sims, M.; Bradley, D. D. C.; Ariu, M.; Koeberg, M.; Asimakis, A.; Grell, M.; Lidzey, D. G. *Adv. Funct. Mater.* **2004**, *14*, 765.
(27) Jain, S.; Bates, F. S. *Science* **2003**, *300*, 460.
(28) (a) Lee, T. A.; Cooper, A.; Apkarian, R. P.; Conticello, V. P. *Adv. Mater.* **2000**, *12*, 1105. (b) Hussain, H.; Busse, K.; Kressler, J. *Macromol. Chem. Phys.* **2003**, *204*, 936.
(29) Wei, Y.; Chan, C. C.; Tian, J.; Jang, C. W.; Hseuh, K. F. *Chem. Mater.* **1991**, *3*, 888.
(30) Zotti, G.; Schiavon, G.; Zecchin, S.; Morin, J.-F.; Leclerc, M. *Macromolecules* **2002**, *35*, 2122.
(31) Brédas, J. L.; Silbey, R.; Boudreaux, D. S.; Chance, R. R. *J. Am. Chem. Soc.* **1983**, *105*, 6555.
(32) (a) Klarner, G.; Lee, J.-I.; Lee, V. Y.; Chan, E.; Chen, J.-P.; Nelson, A.; Markiewicz, D.; Siemens, R.; Scott, J. C.; Miller, R. D. *Chem. Mater.* **1999**, *11*, 1800. (b) Marsitzky, D.; Murray, J.; Scott, J. C.; Carter, K. R. *Chem. Mater.* **2001**, *13*, 4285. (c) Li, Y.; Ding, J.; Day, M.; Tao, Y.; Lu, J.; D'iorio, M. *Chem. Mater.* **2003**, *15*, 4936.
(33) Chen, X.; Liao, J.-L.; Liang, Y.; Ahmed, M. O.; Tseng, H.-E.; Chen, S.-A. *J. Am. Chem. Soc.* **2003**, *125*, 636.
(34) Du, F.-S.; Li, Z.-C.; Hong, W.; Gao, Q.-Y.; Li, F.-M. *J. Polym. Sci., Part A: Polym. Chem.* **2000**, *38*, 679.

MA050267O